Inorg. Chem. **2005**, *44*, 6034–6043

Sulfido-Bridged Dinuclear Molybdenum–Copper Complexes Related to the Active Site of CO Dehydrogenase: $[(dithiolate)Mo(O)S_2Cu(SAr)]^{2-}$ (dithiolate = $1,2\text{-}S_2C_6H_4$, $1,2\text{-}S_2C_6H_2\text{-}3,6\text{-}Cl_2$, $1,2\text{-}S_2C_2H_4$)

Motoki Takuma, Yasuhiro Ohki, and Kazuyuki Tatsumi*

Department of Chemistry, Graduate School of Science and Research Center for Materials Science, Nagoya University, Furo-cho, Chikusa-ku, Nagoya 464-8602, Japan

Received February 25, 2005

The [MoCu] carbon monoxide dehydrogenase (CODH) is a Cu-containing molybdo-flavoprotein, the active site of which contains a pterin-dithiolene cofactor bound to a sulfido-bridged dinuclear Mo–Cu complex. In this paper, the synthesis and characterization of dinuclear Mo–Cu complexes relevant to the active site of [MoCu]-CODH are described. Reaction of $[MoO_2S_2]^{2-}$ with CuCN affords the dinuclear complex $[O_2MoS_2Cu(CN)]^{2-}$ (**1**), in which the CN^- ligand can be replaced with various aryl thiolates to give rise to a series of dinuclear complexes $[O_2MoS_2Cu(SAr)]^{2-}$ (Ar = Ph (**2**), *o*-Tol (**3**), and *p*-Tol (**4**)). An alternative synthesis of complex **2** is the reaction of $[MoO_2S_2]^{2-}$ with $[Cu(SPh)_3]^{2-}$. Similarly, $[O_2MoS_2Cu(PPh_3)]^-$ (**5**), $[O_2MoS_2Cu(dppe)]^-$ (dppe = 1,2-bis(diphenylphosphino)ethane) (**6**), and $[O_2MoS_2Cu(triphos)]^-$ (triphos = 1,1,1-tris[(diphenylphosphino)methyl]ethane) (**7**) were prepared from the reactions of $[MoO_2S_2]^{2-}$ with the Cu(I) phosphine complexes. Treatment of **1**, **2**, **4**, or **5** with dithiols $(1,2\text{-}(SH)_2C_6H_4$, $1,2\text{-}(SH)_2C_6H_2\text{-}3,6\text{-}Cl_2$, and $1,2\text{-}(SH)_2C_2H_4)$, in acetonitrile, leads to the replacement of a molybdenum-bound oxo ligand to yield $[(dithiolate)Mo(O)S_2CuL]^{2-}$ (L = CN, SAr; dithiolate = $1,2\text{-}S_2C_6H_4$, $1,2\text{-}S_2C_6H_2\text{-}3,6\text{-}Cl_2$, or $1,2\text{-}S_2C_2H_4$) (**8**–**13**) or $[(1,2\text{-}S_2C_6H_4)Mo(O)S_2Cu(PPh_3)]^-$ (**14**) complexes.

Introduction

Carbon monoxide dehydrogenase (CODH) in the aerobic bacterium *Oligotropha carboxidovorans* catalyzes the oxidation of CO by H_2O, generating CO_2, two electrons, and two H^+.[1] Recently, the active site has been identified by X-ray crystallography[2] (Figure 1) and extended fine Auger structure (EXAFS)[3] as containing a unique dinuclear Mo−(μ-S)−Cu core. The molybdenum atom is coordinated by a pterin dithiolene cofactor, a hydroxyl group, a terminal oxo ligand, and a sulfide unit which bridges molybdenum to copper. The latter metal is bonded also to a sulfur atom of a cysteine residue. The Mo−Cu distance is 3.70 Å in the oxidized form and increases to 4.23 Å upon reduction. The dinuclear Mo−(μ-S)−Cu fragment is unique to [MoCu]-CODH. Indeed, all of the known molybdoenzymes which contain molybdopterin or molybdopterin dinucleotide units are mononuclear.[4]

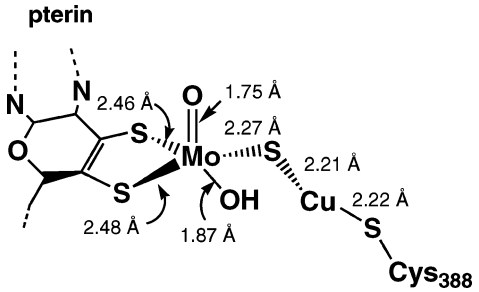

Figure 1. Proposed active site structures of oxidized [MoCu]-CODH, based on X-ray crystallography.[2a]

We can envision two rational routes to synthesize structural models of [MoCu]-CODH. One is the preparation of appropriate molybdenum complexes having oxo and sulfide ligands and a dithiolene moiety, followed by dinucleation with copper thiolate units. The other is the incorporation of a dithiolene group into preorganized dinuclear Mo−Cu

* To whom corresponce should be addressed. E-mail: i45100a@nucc.cc.nagoya-u.ac.jp. Fax: Int.code +81-52-789-2943.

(1) Dobbek, H.; Gremer, L.; Meyer, O.; Huber, R. *Handbook of Metalloproteins*; Messershmidt, A., Huber, R., Poulos, T., Wieghardt, K., Eds.; John Wiley & Sons: New York, 2001; Vol. 2, pp 1136−1147.
(2) (a) Dobbek, H.; Gremer, L.; Kiefersauer, R.; Huber, R.; Meyer, O. *Proc. Natl. Acad. Sci. U.S.A.* **2002**, *99*, 15971. (b) Dobbek, H.; Gremer, L.; Meyer, O.; Huber, R. *Proc. Natl. Acad. Sci. U.S.A.* **1999**, *96*, 8884.
(3) Gnida, M.; Ferner, R.; Gremer, L.; Meyer, O.; Meyer-Klaucke, W. *Biochemistry* **2003**, *42*, 222.
(4) (a) *Molybdenum Enzymes, Cofactors, and Model Systems*; Stiefel, E. I., Coucouvanis, D., Newton, W. E., Eds.; ACS Symposium Series 535; American Chemical Society: Washington, DC, 1993. (b) Enemark, J. H.; Cooney, J. A.; Wang, J. J.; Holm, R. H. *Chem. Rev.* **2004**, *104*, 1157. (c) McMaster, J.; Tunney, J. M.; Garner, C. D. *Prog. Inorg. Chem.* **2004**, *52*, 539−583. (d) Hille, R. *Chem. Rev.* **1996**, *96*, 2757.

10.1021/ic050294v CCC: $30.25
Published on Web 07/29/2005

sulfide complexes. We have chosen the latter strategy since molybdenum sulfide complexes with one dithiolene ligand are unknown.[4a−c] A logical starting point for the construction of the dinuclear Mo−Cu unit is to use simple thiomolybdates, $[MoO_{4-n}S_n]^{2-}$ ($n = 1-4$), since they have remarkable affinity toward transition metals. Thus, the reaction with copper complexes readily takes place to form various types of multinuclear Mo−Cu complexes,[5,6] including dinuclear $[S_2MoS_2Cu(CN)]^{2-}$,[6a,7] $[S_2MoS_2Cu(SAr)]^{2-}$,[8] and $[OSMoS_2Cu(CN)]^{2-}$.[7] Intriguingly, $[MoO_2S_2]^{2-}$ has not yet been utilized in the synthesis of dinuclear Mo−Cu complexes, although the two terminal sulfides on molybdenum are poised to form a sulfido-bridged dinuclear Mo−Cu core, leaving the oxo ligands intact. Possible displacement of one oxo group by a dithiolene group in a second step was inspired by a recent report from Coucouvanis and co-workers[9] who showed that treatment of $[O_2Mo(\mu\text{-}S)_2FeCl_2]^{2-}$ with catechol leads to simple replacement of a Mo=O group with molybdenum−catecholate, as a result of double protonation. Here we describe the successful application of this combined strategy and report that the reaction of $[MoO_2S_2]^{2-}$ with a range of Cu^I complexes gives sulfido-bridged oxo−Mo−Cu complexes. Subsequent treatment of these precursors with dithiols leads to new types of dinuclear sulfido-bridged Mo−Cu complexes having dithiolate ligands, $[(dithiolate)Mo(O)S_2Cu(SAr)]^{2-}$ (dithiolate = benezene-1,2-dithiolate, 3,6-dichloro-benzene-1,2-dithiolate, and 1,2-ethanedithiolate), the structures of which are related to the active site of [MoCu]-CODH.

Results and Discussion

Synthesis of $[O_2MoS_2Cu(CN)]^{2-}$. Treatment of $[MoO_2S_2]^{2-}$ with CuCN in a 1:1 mixture of acetonitrile and CH_2Cl_2 gave, after simple work up, $[O_2MoS_2Cu(CN)]^{2-}$ (**1**) (Scheme 1). Complex **1** is air-stable both in solution and in the solid state and soluble in acetonitrile, methanol, and water. The negative electrospray ionization time of flight mass spectrometry (ESI-TOF-MS) spectrum in acetonitrile clearly shows a set of peaks associated with the parent molecular ion $[O_2MoS_2Cu(CN)]^{2-}$. The observed isotopic pattern matches the theoretical prediction well. The IR spectrum of **1** shows a ν_{CN} band at 2117 cm^{-1}, ν_{MoO} bands at 887 and 862 cm^{-1}, and a $\nu_{\mu\text{-}S}$ band at 449 cm^{-1}. The absorption spectrum of **1** exhibits bands at λ_{max} (ϵ_M), 218 (sh), 278 (7200), 320 (sh), and 402 (1160) nm (Figure 2). The elemental analysis is consistent with the formulation of $(Et_4N)_2[O_2MoS_2Cu(CN)]$. Müller et al. have demonstrated that the terminal sulfide ligands in MoS_4^{2-} readily bind to CuCN to afford both dinuclear $[MoS_4(CuCN)]^{2-}$ and trinuclear $[MoS_4(CuCN)_2]^{2-}$ complexes.[6a] However, the reaction of $[MoO_2S_2]^{2-}$ with CuCN afforded exclusively the dinuclear complex **1**, since the terminal oxo ligands have lower affinity toward late transition metals because of their hard character.

Scheme 1

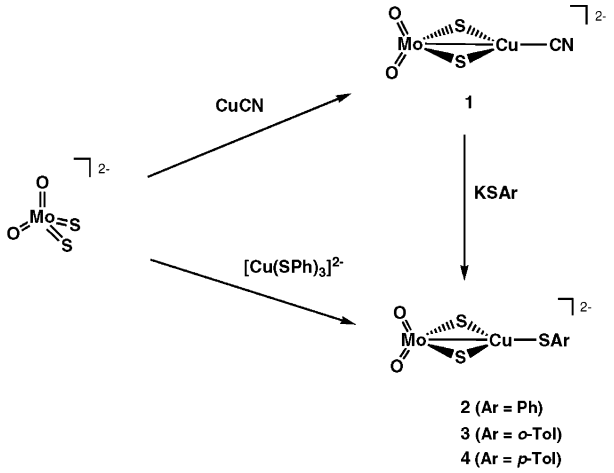

Synthesis and Structures of $[O_2MoS_2Cu(SAr)]^{2-}$ (Ar = Ph (2), *o*-Tol (3), *p*-Tol (4)). The dinuclear Mo−Cu−SAr complexes, **2**−**4**, are closely analogous to $[S_2MoS_2Cu(SAr)]^{2-}$ described by Garner and Clegg.[8] Following the synthetic procedure for $[S_2MoS_2Cu(SAr)]^{2-}$, $[O_2MoS_2Cu(SAr)]^{2-}$ (Ar = Ph (**2**), *o*-Tol (**3**), or *p*-Tol (**4**)) was obtained in high yields from the reaction between $[O_2MoS_2Cu(CN)]^{2-}$ and KSAr (Scheme 1). An alternative synthesis of the benzenethiolate derivative **2** is the reaction of $(Et_4N)_2[MoO_2S_2]$ with $(Et_4N)_2[Cu(SPh)_3]$ in acetonitrile. Complexes

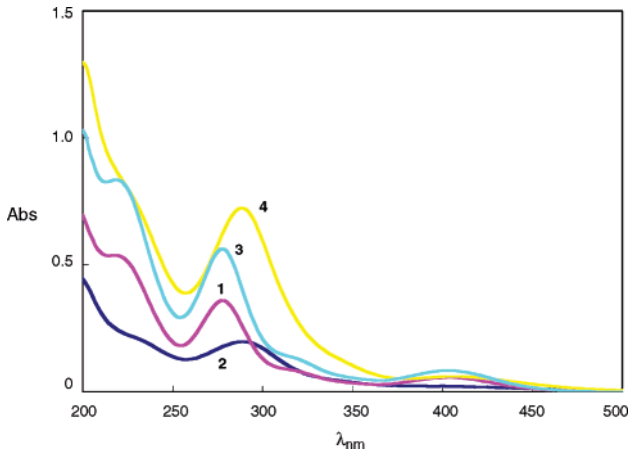

Figure 2. UV−vis spectra of **1** (purple), **2** (blue), **3** (light blue), and **4** (yellow) in acetonitrile.

(5) Müller, A.; Diemann, E.; Jostes, R.; Bögge, H. *Angew. Chem., Int. Ed. Engl.* **1981**, *20*, 934.
(6) (a) Müller, A.; Dartmann, M.; Römer, C.; Clegg, W.; Sheldrick, G. M. *Angew. Chem., Int. Ed. Engl.* **1981**, *20*, 1060. (b) Müller, A.; Bögge, H.; Tölle, H. G.; Jostes, R.; Schimanski, U.; Dartmann, M. *Angew. Chem., Int. Ed. Engl.* **1981**, *19*, 654. (c) Li, Z.; Du, S.; Wu, X. *Inorg. Chem.* **2004**, *43*, 4776. (d) Huang, Q.; Wu, X.; Wang, Q.; Sheng, T.; Lu, J. *Inorg. Chem.* **1996**, *35*, 893. (e) Müller, A.; Bögge, H.; Tölle, H. G.; Joster, R.; Scimanski, U.; Dartmann, M. *J. Chem. Soc., Chem. Commun.* **1980**, 91. (f) Nicholson, J. R.; Flood, A. C.; Garner, C. D.; Clegg, W. *J. Chem. Soc., Chem. Commun.* **1983**, 1179. (g) Secheresse, F.; Manoli, J. M.; Potvin, C.; Marzak, S. *J. Chem. Soc., Dalton Trans.* **1988**, 3055. (h) Potvin, C.; Manoli, J. M.; Salis, M.; Secheresse, F. *Inorg. Chim. Acta* **1984**, *83*, L19. (i) Lei, X.-J.; Huang, Z.-Y.; Liu, Q.-T.; Hong, M.-C.; Liu, H.-Q. *Inorg. Chem.* **1989**, *28*, 4302. (j) Lei, X.-J.; Huang, Z.-Y.; Yu, K.-B. *J. Chem. Soc., Chem. Commun.* **1991**, 249. (k) Du, S.-W.; Zhu, N.-Y.; Chen, P.-C.; Wu, X.-T. *Angew. Chem., Int. Ed. Engl.* **1992**, *8*, 31. (l) Guo, G.-C.; Kwok, R. W. M.; Mak, T. C. W. *Inorg. Chem.* **1997**, *36*, 2475.
(7) Gheller, S. T.; Hambley, T. R.; Rodgers, J. R.; Brownlee, R. T. C.; O'Connnor, M. J.; Snow, M. R.; Wedd, A. G. *Inorg. Chem.* **1984**, *23*, 2519.
(8) Acott, S. R.; Garner, D.; Nicholson, J. R.; Clegg, W. *J. Chem. Soc., Dalton Trans.* **1983**, 713.
(9) Han, J.; Koutmos, M.; Ahmad, S. A.; Coucouvanis, D. *Inorg. Chem.* **2001**, *40*, 5985.

Table 1. Selected Bond Lengths (Å) and Angles (deg) for **2**, **3**, and **4**

	2	3	4
Mo−Cu	2.6598(8)	2.654(1)	2.654(1)
Mo−O1	1.733(5)	1.779(8)	1.714(5)
Mo−O2	1.732(5)	1.727(8)	1.720(5)
Mo−S1	2.268(2)	2.252(2)	2.266(2)
Mo−S2	2.256(2)	2.271(2)	2.253(2)
Cu−S1	2.220(2)	2.240(2)	2.220(2)
Cu−S2	2.231(2)	2.212(3)	2.228(2)
Cu−S3	2.191(2)	2.183(3)	2.179(2)
S1−Mo−S2	106.04(6)	106.17(9)	106.15(6)
S1−Mo−O1	110.2(2)	111.4(3)	110.1(2)
S1−Mo−O2	110.1(2)	111.0(3)	110.3(2)
S1−Cu−S2	108.51(6)	108.66(10)	108.59(7)

2−**4** are soluble in acetonitrile, methanol, and water but insoluble in relatively nonpolar solvents such as tetrahydrofuran (THF) and diethyl ether. In contrast to **1**, complexes **2**−**4** are highly hygroscopic and exposure of the solids to air leads to immediate deliquescence. The IR spectra of **2**−**4** are similar and that of **2** exhibits characteristic strong bands at 893 and 870 cm^{-1} for ν_{MoO} and 455 cm^{-1} for $\nu_{\mu\text{-}S}$. The ν_{MoO} bands of **2**−**4** are at higher frequencies than those for $(Et_4N)_2[MoO_2S_2]$ (860 and 840 cm^{-1}). The reason for this is that the anticipated reduction in electron density at molybdenum, because of the change from terminal Mo═S groups in $(Et_4N)_2[MoO_2S_2]$ to two Mo−(μ-S)−Cu in **2**−**4**, is compensated by stronger π-donation from the terminal oxo ligands and stronger Mo═O bonds in the latter complexes. The UV−vis spectrum of **2**−**4** in acetonitrile shows an intense band at 270−290 nm and a broad absorption around 400 nm with additional shoulders, more or less resolved depending on the complex, around 220 and 320 nm (Figure 2). The intense band in 270−290 nm is attributed to a ligand-to-metal charge-transfer transition (LMCT) of the MoO_2S_2 moiety perturbed by coordination to the (ArS)Cu moiety, since $[MoO_2S_2]^{2-}$ exhibits strong absorptions at 321 and 388 nm.[10] The shoulders around 220 and 320 nm are tentatively assigned to the charge-transfer transitions from sulfur to copper, in comparison with those of $[S_2MoS_2Cu(SPh)]^{2-}$ observed at 240 and 350 nm.[8]

The solid-state structures of three complexes, **2**−**4**, were determined by single-crystal X-ray diffraction. Selected bond lengths and angles of **2**, **3**, and **4** are listed in Table 1. Since complexes **2**, **3**, and **4** are isomorphous, only the structure of **2** (Figure 3) is discussed below. The copper atom is bonded to a benzenethiolate ligand and two bridging sulfides, forming a trigonal planar geometry with (μ-S)−Cu−(μ-S) angle of 108.51(6)°. The Cu−SPh distance, 2.191(2) Å, is shorter than those for $(Et_4N)_2[Cu(SPh)_3]$ (2.253(2), 2.258(2), and 2.239(2) Å),[11] probably because of a less crowded environment for copper. The Cu−(μ-S) lengths of 2.220(2) and 2.231(2) Å are slightly longer than the Cu−SPh distance. The molybdenum atom is tetrahedrally coordinated by two terminal oxo and two bridging sulfide ligands. The Mo−(μ-S) distances (2.268(2) and 2.256(2) Å) are comparable

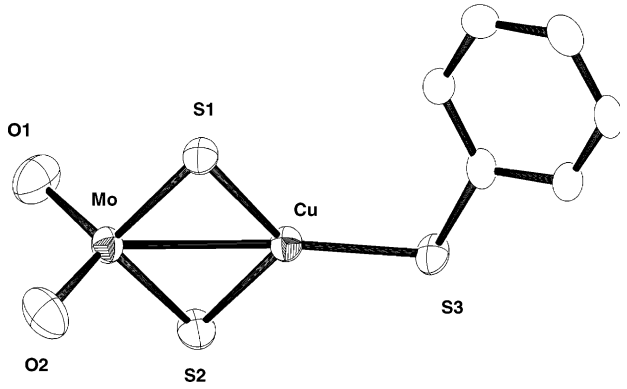

Figure 3. ORTEP drawing of the complex anion, **2**.

Scheme 2

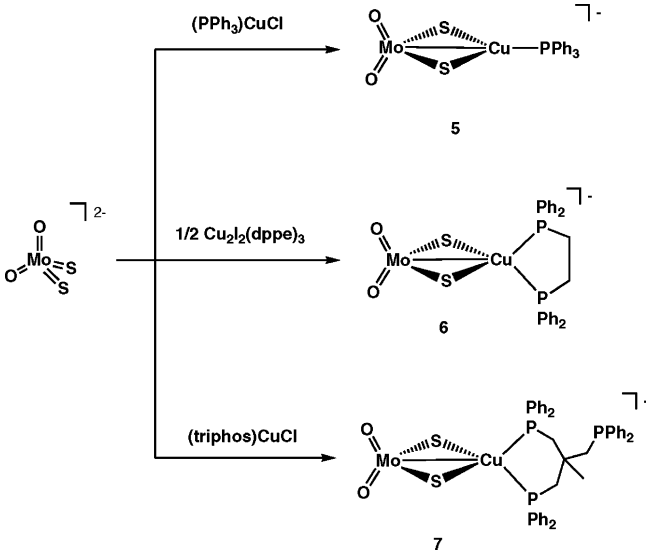

to those in $[S_2MoS_2Cu(SPh)]^{2-}$ (2.227(2) and 2.214(2) Å).[8] The two Mo═O distances, 1.733(5) and 1.732(5) Å, are longer than the Mo═O bonds in $MoO_2(OSiPh_3)_2$ (1.692(7) Å)[12] and MoO_2(O-2,4,6-*t*-$Bu_3C_6H_2)_2$ (1.682(2) Å).[13] This is in agreement with the lower Mo═O stretching frequency of **2** than those of siloxy and aryloxide complexes (930−965 cm^{-1}).[12,13] The Mo−Cu distance of 2.6598(8) Å is close to that for $[S_2MoS_2Cu(SPh)]^{2-}$ (2.636(1) Å).[8] These Mo−Cu distances could be indicative of a direct metal−metal interaction,[8] such as dative bonding from d^{10} Cu(I) to d^0 Mo(VI).

Reaction of $[MoO_2S_2]^{2-}$ with Cu(I) Phosphine Complexes. The addition of $(PPh_3)CuCl$, $Cu_2I_2(dppe)_3$, or (triphos)CuCl to an acetonitrile solution of $[MoO_2S_2]^{2-}$ afforded $[O_2MoS_2Cu(PPh_3)]^-$ (**5**), $[O_2MoS_2Cu(dppe)]^-$ (**6**), and $[O_2MoS_2Cu(triphos)]^-$ (**7**), respectively (Scheme 2). Electronic spectra of **5**−**7** in acetonitrile displayed an intense band at 270−280 nm, with a shoulder between 310 and 320 nm, and a moderate absorption in 380−450 nm (Figure 4). As with **1**−**4**, the absorption band in 270−280 nm is ascribed to LMCT transition of the MoO_2S_2 fragments. In the IR spectra, the ν_{MoO} bands and the $\nu_{\mu\text{-}S}$ bands of **5** (899, 868,

(10) McDonald, J. H.; Friesen, G. D.; Rosenhein, L. D.; Newton, W. *Inorg. Chim. Acta* **1983**, *72*, 205.
(11) Garner, C. D.; Nicholson, J. R.; Clegg, W. *Inorg. Chem.* **1984**, *23*, 2148.
(12) Huang, M.; Dekock, C. W. *Inorg. Chem.* **1993**, *32*, 2287.
(13) Hanna, T. A.; Ghosh, A. K.; Ibarra, C.; Mendez-Rojas, M. A.; Rheingold, A. L.; Watson, W. H. *Inorg. Chem.* **2004**, *43*, 1511.

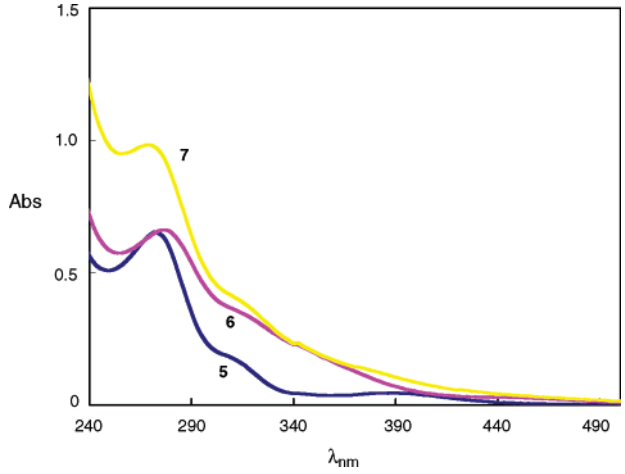

Figure 4. UV−vis spectra of **5** (blue), **6** (purple), and **7** (yellow) in acetonitrile.

Table 2. Selected Bond Lengths (Å) and Angles (deg) for **5**, **6**, and **7**

	5	**6**	**7**
Mo−Cu	2.6769(8)	2.7267(2)	2.754(1)
Mo−O1	1.736(3)	1.726(1)	1.724(5)
Mo−O2	1.720(3)	1.736(1)	1.773(7)
Mo−S1	2.262(1)	2.2513(5)	2.254(2)
Mo−S2	2.2681(9)	2.2476(4)	2.250(2)
Cu−S1	2.233(1)	2.2990(5)	2.295(2)
Cu−S2	2.207(1)	2.2884(5)	2.309(2)
Cu−P1	2.204(1)	2.2584(4)	2.249(2)
Cu−P2		2.3614(5)	2.303(2)
S1−Mo−S2	105.09(3)	106.88(2)	106.58(7)
S1−Mo−O1	109.18(9)	109.54(5)	109.8(2)
S1−Mo−O2	109.33(9)	110.43(5)	109.7(2)
S1−Cu−S2	108.20(4)	103.95(2)	103.29(8)
S(1)−Cu−P(1)	122.47(5)	122.48(2)	118.24(7)
S(2)−Cu−P(2)		109.90(2)	104.94(8)
P(1)−Cu−P(2)		89.03(2)	100.20(7)

and 455 cm^{-1}), **6** (887, 864, and 453 cm^{-1}), and **7** (887, 870, and 449 cm^{-1}) are close to those for **1** and **2**−**4** described above. This indicates that the Mo═O and Mo−(μ-S)−Cu interactions are not influenced as much by the ligand and the geometry at the copper site.

The molecular structures of **5**−**7** are presented in Figures S3, S4, and 5, respectively, and important bond lengths and angles are listed in Table 2. The structures reveal sulfido-bridged dinuclear complexes consisting of a tetrahedral MoO_2S_2 unit and a trigonal planar (**5**) or trigonal pyramidal (**6** and **7**) copper center. The structure of **5** is geometrically analogous to **2**−**4**; thus the Mo−Cu distance of 2.6769(8) Å (**5**) is similar to those of **2** (2.6598(8) Å) and $[O_2MoS_2$-$CuS(o\text{-Tol})]^{2-}$ (**3**) (2.654(1) Å). The diphosphine complex **6** and triphosphine complex **7** contain four-coordinate copper centers, and exhibit longer Cu−S distances (2.2884(5)−2.309(2) Å) than those of **5** (2.207(1) and 2.233(1) Å), which result in longer Mo−Cu distances of 2.7267(2) Å (**6**) and 2.754(1) Å (**7**). The geometries of copper in **6** and **7** are very distorted from tetrahedral and are almost better described as trigonal pyramidal having P(2) at the apical position and S(1), S(2), and P(1) at basal positions. As a consequence, the apical Cu−P2 distances (2.3614(5) Å (**6**) and 2.303(2) Å (**7**)) are notably longer than the Cu−P1 distances, 2.2584(4) Å (**6**) and 2.249(2) Å (**7**).

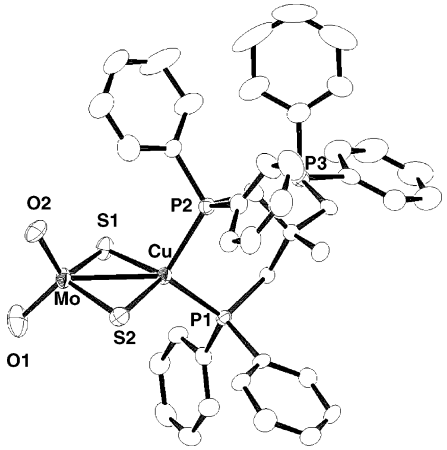

Figure 5. ORTEP drawing of the complex anion, **7**.

Replacement of an Oxo ligand in $[O_2MoS_2CuL]^{2-}$ (L = CN, SAr) or $[O_2MoS_2Cu(PPh_3)]^-$ with Dithiolates: Synthesis of Structural Models for the Active Site of [MoCu]-CODH. Protonation of an oxo ligand of the Mo−Cu sulfide complexes with dithiols turned out to be an effective way for replacing a terminal oxo ligand with a dithiolate. Treatment of an acetonitrile solution of **1**, **2**, and **4** with benzene-1,2-dithiol over the course of 4 h afforded the $[(1,2\text{-}S_2C_6H_4)Mo(O)S_2CuL]^{2-}$ complexes **8**−**10**, as summarized in Scheme 3. The analogous dithiolate derivatives **11** and **12** and $[(1,2\text{-}S_2C_2H_4)Mo(O)S_2Cu(SPh)]^{2-}$ (**13**) were prepared in a similar manner using 3,6-dichloro-benzene-1,2-dithiol and 1,2-ethanedithiol. Incorporation of benzenedithiolate was also successful using the phosphine complex **5**. The product, ascribed to $[(1,2\text{-}S_2C_6H_4)Mo(O)S_2Cu(PPh_3)]^-$ (**14**), was observed in the ESI-TOF-MS spectrum. However, the treatment of diphosphine complex **6** with benzene-1,2-dithiol resulted in the formation of a complex mixture.

These complexes are the first examples of sulfido-bridged dinuclear Mo−Cu complexes having a dithiolate group bound to molybdenum, although mononuclear molybdenum oxo complexes having a dithiolate ligand such as $[MoO_2(SC_6H_2\text{-}2,4,6\text{-}{}^iPr_3)(1,2\text{-}S_2C_6H_4)]^-$,[14a] $[MoO_2(OSiPh_3)(1,2\text{-}S_2C_6H_4)]^-$,[14a] and $[MoO_3(1,2\text{-}S_2C_6H_4)]^{2-}$,[14b] have been prepared in relation to the molybdopterin cofactor, xanthine oxidase, and sulfite oxidase. The substitution reaction described here is due to double protonation of a terminal oxo ligand by the dithiol and represents an extension of the procedure reported by Coucouvanis and co-workers.[9] They have demonstrated that treatment of $[O_2Mo(\mu\text{-}S)_2FeCl_2]^{2-}$ with cathecol leads to protonation of an oxoligand, generating water and a Mo−Fe catecholate complex.[9] The dinuclear complexes **8**−**13** were characterized on the basis of the IR spectra, ESI-TOF-MS spectra, and elemental analyses. The negative ion mass spectra of **8**−**14** in acetonitrile clearly showed sets of peaks, the isotopic patterns of which matched the calculated isotope patterns well. The IR spectrum of **8** exhibits a ν_{CN} band at 2119 cm^{-1}, a ν_{MoO} band at 924 cm^{-1}, and a $\nu_{\mu\text{-}S}$ band at 426 cm^{-1}, respectively. Complexes **9**−**13** exhibited ν_{MoO} and $\nu_{\mu\text{-}S}$ stretching bands in the same regions.

(14) (a) Lim, B. S.; Willer, M. W.; Miao, M.; Holm, R. H. *J. Am. Chem. Soc.* **2001**, *123*, 8343. (b) Partyka, D. V.; Holm, R. H. *Inorg. Chem.* **2004**, *43*, 8609.

Scheme 3

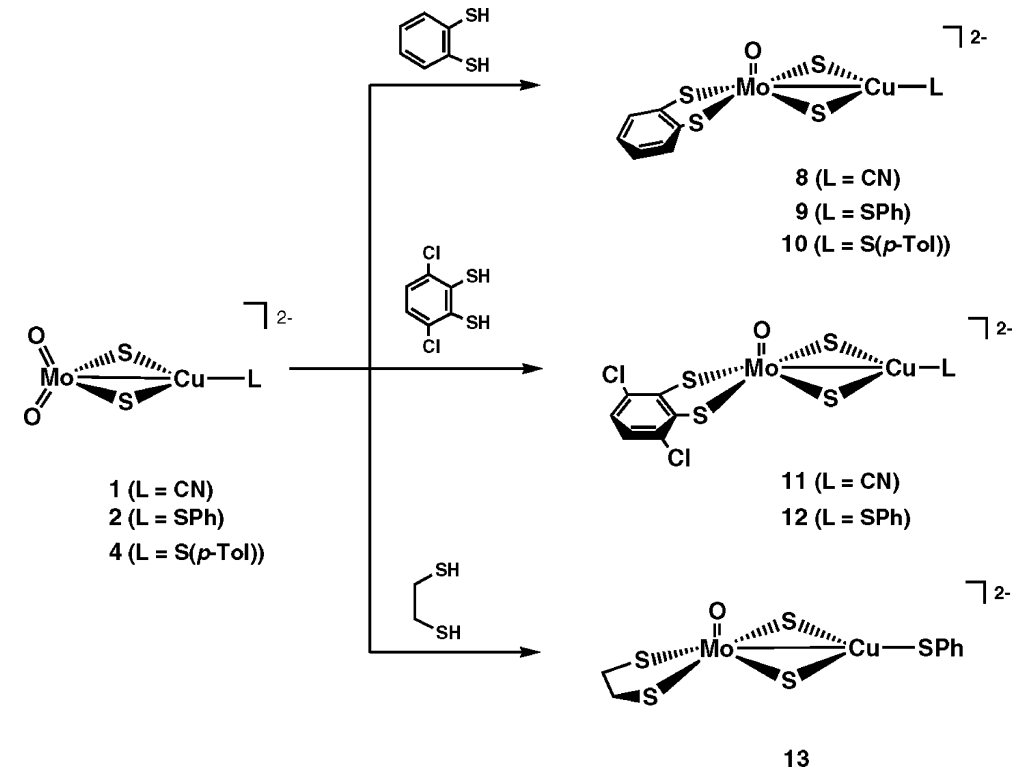

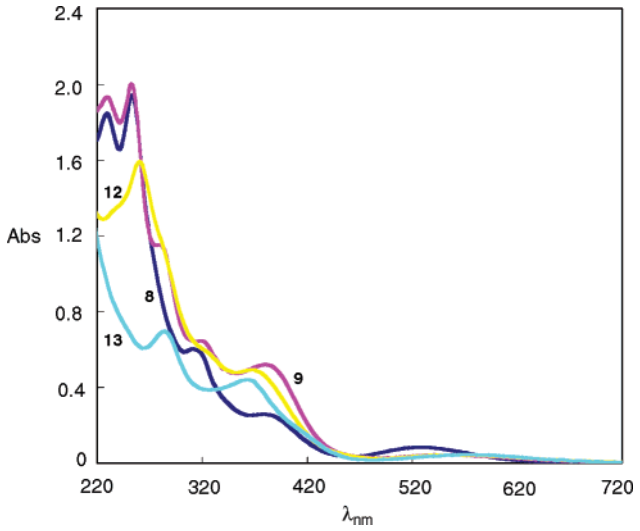

Figure 6. UV−vis spectra of **8** (blue), **9** (purple), **12** (yellow), and **13** (light blue) in acetonitrile.

Incorporation of a dithiolate ligand increased the frequency of the Mo=O vibration from 887 and 862 cm^{-1} in complex **1** and to 924 cm^{-1} in complex **8**, whereas the $\nu_{\mu\text{-S}}$ decreased from 449 (**1**) to 426 cm^{-1} (**8**). The electronic spectrum of complexes **8**, **9**, **12**, and **13** is shown in Figure 6. Complexes **8** and **9** exhibit absorption bands at 230 and 252−254 nm and a shoulder decending into lower energy in 310−320 nm, whereas **12** exhibits similar bands at 238 (sh) and 260 nm but no absorption around 310 nm. The characteristic absorptions, around 400 nm and above 500 nm, are common for **8**−**13**. The latter transition is assignable to a charge transfer from dithiolate to molybdenum, since in xanthine oxidase a similar band was observed at 580 nm.[15]

Table 3. Redox Properties of (dithiolate)Mo(VI)−Cu(I) Complexes

complex	$E_{1/2}$ or E_{pc}, V^a	
$[(1,2\text{-}S_2C_6H_4)Mo(O)S_2Cu(CN)]^{2-}$ (**8**)	−2.02	−1.23
$[(1,2\text{-}S_2C_6H_2\text{−}3,6\text{-}Cl_2)Mo(O)S_2Cu(CN)]^{2-}$ (**11**)	−1.95	−1.18
$[(1,2\text{-}S_2C_6H_4)Mo(O)S_2Cu(SPh)]^{2-}$ (**9**)	−2.10[b]	−1.29[b]
$[(1,2\text{-}S_2C_6H_4)Mo(O)S_2CuS(p\text{-Tol})]^{2-}$ (**10**)	−2.13[b]	−1.32[b]
$[(1,2\text{-}S_2C_2H_4)Mo(O)S_2Cu(SPh)]^{2-}$ (**15**)	−2.33[b]	

[a] $E_{1/2} = (E_{pa} + E_{pc})/2$, 100 mV, vs Ag/Ag^+. [b] Irreversible, E_{pc}.

Electrochemistry. The redox properties of $[(dithiolate)Mo(O)S_2CuL]^{2-}$ complexes have been examined by cyclic voltammetry (CV) in acetonitrile at room temperature (Table 3). The cyclic voltammogram of **8** exhibits quasi-reversible processes at $E_{1/2} = -2.02$ and −1.23 V vs Ag/Ag^+ (Figure S8), which are ascribed to one-electron reductions to the corresponding $[(1,2\text{-}S_2C_6H_4)Mo(O)S_2Cu(CN)]^{3-}$ and $[(1,2\text{-}S_2C_6H_4)Mo(O)S_2Cu(CN)]^{4-}$ species, respectively. A similar result was obtained for **11**, showing two reduction waves at $E_{1/2} = -1.95$ and −1.18 V (Figure S11). The obvious reduction site is at molybdenum, and the redox behavior is interpreted as $Mo^{VI}/Mo^{V}/Mo^{IV}$ processes perturbed by the dithiolate ligand and the copper unit. Although the redox potentials, and the Mo=O stretching frequency, were previously reported to be influenced by the electronic property of the dithiolate ligand in $[MoO(dithiolate)_2]^{2-}$ (dithiolate = $S_2C_2H_2$, $S_2C_2(CN)_2$, $1,2\text{-}S_2C_6H_4$),[16] the nature of the dithiolate ligand in our dinuclear complexes was found not to have an effect. However, the reversibility of the reduction processes is affected by the ligand on copper. The Cu−CN complex, **8**, exhibits two quasi-reversible reduction waves

(15) (a) Garbett, K.; Gillard, R. D.; Knowles, P. F.; Stangroom, J. E. *Nature* **1967**, *215*, 824. (b) Boyd, I. W.; Dance, I. G.; Murray, K. S.; Wedd, A. G. *Aust. J. Chem.* **1978**, *31*, 279.

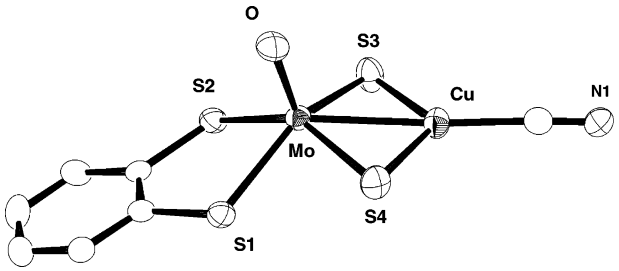

Figure 7. ORTEP drawing of the complex anion, **8**.

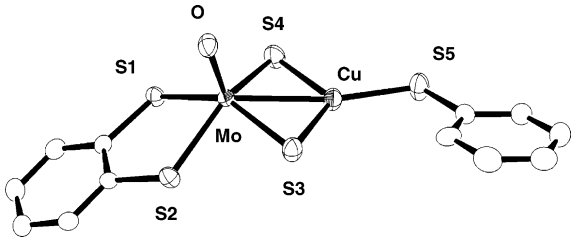

Figure 8. ORTEP drawing of the complex anion, **9**.

Table 4. Selected Bond Lengths (Å) and Angles (deg) for (dithiolate)Mo−Cu Complexes **8**−**10**, **12**, and **13**

	8	**9**	**10**	**12**	**13**
Mo−Cu	2.599(1)	2.596(1)	2.583(2)	2.5977(8)	2.602(2)
Mo═O	1.694(4)	1.700(4)	1.687(4)	1.687(4)	1.692(8)
Mo−S1	2.434(2)	2.446(2)	2.434(2)	2.439(2)	2.451(3)
Mo−S2	2.448(2)	2.445(2)	2.447(2)	2.432(2)	2.445(4)
Mo−S3	2.306(2)	2.309(2)	2.323(2)	2.298(2)	2.324(3)
Mo−S4	2.307(2)	2.302(2)	2.302(2)	2.313(2)	2.297(4)
Cu−S3	2.181(2)	2.168(2)	2.174(2)	2.191(2)	2.178(4)
Cu−S4	2.180(2)	2.174(2)	2.175(2)	2.176(2)	2.189(3)
Cu−S5		2.164(2)	2.170(2)	2.178(2)	2.180(4)
S1−Mo−S2	80.19(5)	80.47(6)	79.55(5)	80.71(6)	79.9(1)
S3−Mo−S4	104.03(6)	103.96(7)	104.28(7)	103.90(6)	104.1(1)
S1−Mo−S3	146.03(6)	146.92(7)	147.29(6)	142.63(6)	150.9(1)
S2−Mo−S4	146.54(5)	146.68(7)	144.00(6)	150.04(6)	104.1(1)
S3−Cu−S4	112.99(7)	113.58(8)	114.20(7)	112.52(7)	113.1(1)

while the CV spectrum of **9** shows two irreversible reduction peaks at $E_{pc} = -2.10$ and -1.29 V (Figure S9). Upon reduction, the SPh ligand may become labile because of electronic repulsion, whereas the CN ligand, behaving as a good π-acceptor, stabilizes the reduced states.

Structures of the [(dithiolate)Mo(O)S_2CuL]$^{2-}$ Complexes: [(1,2-$S_2C_6H_4$)Mo(O)S_2CuL]$^{2-}$ (L = CN (8), SPh (9), S(*p*-Tol) (10)), [(1,2-$S_2C_6H_2$-3,6-Cl_2)Mo(O)S_2Cu(SPh)]$^{2-}$ (12), and [(1,2-$S_2C_2H_4$)Mo(O)S_2Cu(SPh)]$^{2-}$ (13). The molecular structures of isostructural complexes **8**−**10**, **12**, and **13** were determined by X-ray diffraction studies. Representative drawings of **8** and **9** are depicted in Figure 7 (for **8**) and Figure 8 (for **9**), and selected bond lengths and angles are summarized in Table 4. The dinuclear Mo−Cu complexes comprise important structural features of [MoCu]-CODH. The molybdenum atom adopts a square pyramidal geometry and is bonded to a terminal oxoligand at the apical position; a dithiolate and two bridging sulfide ligands occupy the basal positions. The 1,2-$S_2C_6H_4$, 1,2-$S_2C_6H_2$-3,6-Cl_2, and 1,2-$S_2C_2H_4$ ligands provide a coordination mode similar to the dithiolene group in CODH, such that the Mo−S distances of **9** (2.446(2) and 2.445(2) Å), **12** (2.439(2) and 2.432(2) Å), and **13** (2.451(3) and 2.445(4) Å) are very close to those determined for the oxidized form of [MoCu]-CODH (2.46 and 2.48 Å).[2a] The Mo−(μ-S) distances (2.309(2) and 2.302(2) Å) and the Mo═O length (1.700(4) Å) of **9** are also similar to those of [MoCu]-CODH (Mo−(μ-S), 2.27 Å; Mo═O, 1.75 Å).[2a] The Mo═O distances of our model complexes (1.687(4) −1.700(4) Å) are in the range of those reported for oxo-molybdenum(VI) complexes.[12,13,14a] The copper atom is bound to a thiolate ligand and the two bridging sulfides in a trigonal planar geometry. The Cu−SAr and Cu−(μ-S) bond distances of **9**, **10**, **12**, and **13** (av 2.17 and 2.18 Å, respectively) are similar, and are comparable, to those in [MoCu]-CODH, Cu−S(Cys) (2.22 Å) and Cu−(μ-S) (2.21 Å). The notable differences between the model complexes and the active site of [MoCu]-CODH are the number of bridging sulfides and the geometry around copper. The second bridging sulfide in our compounds brings the two metals closer; therefore the Mo−Cu distances (2.583(2)−2.602(2) Å) in the dinuclear complexes are significantly shorter than that in the oxidized form of [MoCu]-CODH (3.70 Å).

Reaction of 9 with CO and ^{t}BuNC. The enzymatic reaction mediated by CODH resembles the water−gas shift reaction, where CO and water are transformed into CO_2 and H_2. Thus, homogeneous catalysts for the water−gas shift reaction are of relevance to the enzymatic process.[17] Following the pioneering work by Ford on ruthenium carbonyls,[18] various metal carbonyls,[19] carbonyl cluster compounds,[20] and some phosphine complexes,[21] in combination with acids or bases, have been found to catalyze the water−gas shift reaction. However, the sulfido-bridged dinuclear structure of [MoCu]-CODH is quite unique in comparison to the known homogeneous catalysts. Recently, Dobbek et al. have demonstrated that the action of [MoCu]-CODH is inhibited by *n*-butylisocyanide. The result of the reaction is the formation of an imino(thio)carbonate linkage between molybdenum and copper, with a four membered ring consisting of Mo, S, C, and O (Figure 9).[2a] Attempts to mimic the reaction of [MoCu]-CODH with isocyanide and CO using the complexes reported herein were unsuccessful. No reaction was observed when **9** was treated with an excess of ^{t}BuNC, even under reflux in acetonitrile. Although the color of an acetonitrile solution of **9** under 10 atm of CO at room temperature gradually changed from purple to yellow, the

(16) (a) Lim, B. S.; Donahue, J. P.; Holm, R. H. *Inorg. Chem*. **2000**, *39*, 263. (b) Donahue, J. P.; Goldsmith, C. R.; Nadiminti, U.; Holm, R. H. *J. Am. Chem. Soc*. **1998**, *120*, 12869.

(17) Crabtree, R. H. *The Organometallic Chemistry of the Transition Metals*; John Wiley & Sons: New York, 2001; pp 494−498.

(18) (a) Ford, P. C. *Acc. Chem. Res.* **1981**, *14*, 31. (b) Laine, R. M.; Rinker, R. G.; Ford, P. C. *J. Am. Chem. Soc*. **1977**, *99*, 252.

(19) (a) Chen, C. H.; Hendriksen, D. E.; Eisenberg, R. *J. Am. Chem. Soc*. **1977**, *99*, 2791. (b) King, R. B.; Frazier, C. C.; Hanes, R. M.; King, A. D. *J. Am. Chem. Soc*. **1978**, *100*, 2925.

(20) (a) Kang, H.; Mauldin, C. H.; Cole, T.; Slegeir, W.; Cann, K.; Pettit, R. *J. Am. Chem. Soc*. **1977**, *99*, 8323. (b) Ford, P. C.; Rinker, R. G.; Ungermann, C.; Laine, R. M.; Landis, V.; Moya, S. A. *J. Am. Chem. Soc*. **1978**, *100*, 4595. (c) Ungermann, C.; Landis, V.; Moya, S.; Cohen, H.; Walker, H.; Pearson, R. G.; Rinker, R. G.; Ford, P. C. *J. Am. Chem. Soc*. **1979**, *101*, 5922. (d) Fachinetti, G.; Funaioli, T.; Lecci, L.; Marchetti, F. *Inorg. Chem*. **1996**, *35*, 7217. (e) Fachinetti, G.; Fochi, G.; Funaioli, T. *Inorg. Chem.* **1994**, *33*, 1719.

(21) (a) Yoshida, T.; Ueda, Y.; Otsuka, S. *J. Am. Chem. Soc*. **1978**, *100*, 3941. (b) Yoshida, T.; Okano, T.; Ueda, Y.; Otsuka, S. *J. Am. Chem. Soc*. **1981**, *103*, 3411.

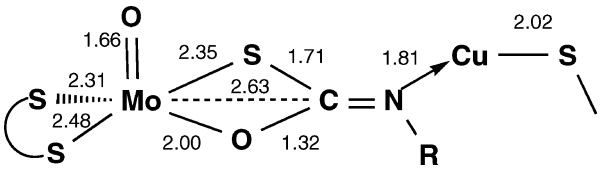

Figure 9. Structure of the *n*-butylisocyanide inhibited form of [MoCu]-CODH.[2a]

IR spectrum of the resulting yellow product exhibited several peaks in the $\nu_{Mo=O}$ region but no band assignable to a bridging sulfide or CO ligand. A similar yellow solid was also obtained when CO treatment of **9** was carried out in the presence of base and water. Thus, coordination of CO at the copper site appears to be followed by fragmentation to give a complex mixture. Presumably, the disulfido-bridged geometry of dinuclear Mo−Cu complexes prevents insertion of isocyanide or CO into a Cu−S bond, possibly because in the putative isocyanide- or CO-bound intermediate the copper center is tetrahedral or trigonal pyramidal.

Conclusions

Dithiomolybdate $[MoO_2S_2]^{2-}$ was found to be a versatile precursor for the construction of sulfido-bridged dinuclear Mo−Cu complexes. Electrophilic substitution, via double protonation of an oxo ligand in $O_2Mo^{VI}(\mu\text{-}S)_2Cu^{I}$, proved to be a useful and effective synthetic approach to the preparation of dinuclear complexes having a dithiolate and an oxo ligand. The dinuclear Mo−Cu complexes so obtained comprise important features of the active site of [MoCu]-CODH, such as a square-pyramidal molybdenum with an apical oxo ligand, a dinuclear framework bridged by sulfur, and a dithiolate ligand on molybdenum mimicking the pterin dithiolene cofactor.

Experimental Section

General Procedures. All of the reactions were carried out using standard Schlenk technique under a N_2 atmosphere. Solvents were dried, degassed, and distilled from sodium/benzophenone ketyl (THF, Et_2O) or from CaH_2 (acetonitrile, CH_2Cl_2, methanol) under nitrogen. ^{t}BuOMe was stored over 4-Å molecular sieves. Deuterated solvents were vaccum transferred from CaH_2 (acetonitrile) under nitrogen or stored over 4 Å molecular sieves (dimethylsulfoxide (DMSO)).

^{1}H NMR spectra were acquired on a Varian INOVA-500 spectrometer at 500 MHz or a JEOL ECA600 spectrometer at 600 MHz. ^{31}P NMR spectra were acquired on a Varian INOVA-500 spectrometer at 202 MHz. ^{1}H NMR spectra were referenced to the residual proton resonances of the deuterated solvents. ^{31}P chemical shifts were relative to the external reference of 85% H_3PO_4. IR spectra were recorded on a JASCO FT/IR-410 spectrometer. UV−vis spectra were measured using a JASCO V560 spectrometer. ESI-TOF-MS spectra were obtained from a Micromass LCT TOF-MS spectrometer. Elemental analyses for C, H, N, and S were performed on a LECO CHNS-932 elemental analyzer on crystalline samples sealed in silver capsules under argon. Cyclic voltammograms were recorded in acetonitrile using a Pt working electrode with 0.2 M $(Bu_4N)(PF_6)$ as the supporting electrolyte. The potential is reported with respect to an $Ag/AgNO_3$ nonaqueous reference electrode filled with acetonitrile and $(Bu_4N)(PF_6)$. X-ray diffraction data were collected on an AFC7R/Mercury CCD system, an AFC8/Saturn 70 CCD system, and a RA-Micro7/Saturn 70 with a MicroMax-007 system using graphite-monochromated Mo Kα radiation.

The following compounds were prepared according to the literature procedures: $(Et_4N)_2[MoO_2S_2]$,[10] $(Et_4N)_2[Cu(SPh)_3]$,[11] $(PPh_3)CuCl$,[22] $Cu_2I_2(dppe)_3$ (dppe = 1,2-bis(diphenylphosphino)-ethane),[23] and (triphos)CuCl (triphos = 1,1,1-tris[(diphenylphosphino)methyl]ethane).[24]

$(Et_4N)_2[O_2MoS_2Cu(CN)]$ ($(Et_4N)_2$[1]). To a solution of $(Et_4N)_2[MoO_2S_2]$ (2.07 g, 4.6 mmol) in 25 mL of acetonitrile was added a suspension of CuCN (0.429 g, 4.8 mmol) in 25 mL of CH_2Cl_2. The reaction mixture was centrifuged to remove some insoluble materials after stirring for 4 h. The supernatant was diluted with 80 mL of diethyl ether to precipitate a yellow-orange powder of ($(Et_4N)_2$(**1**)) (2.28 g, 92%). The product was recrystallized from acetonitrile/Et_2O. IR (KBr, cm^{-1}): ν(CN) 2117, ν(Mo═O) 887, 862, ν(Mo−S−Cu) 449. UV−vis (λ_{max}, nm (ϵ, M^{-1} cm^{-1}), acetonitrile): 218 (sh), 278 (7200), 320 (sh), 402 (1160). ESI-TOF-MS (acetonitrile): *m*/*z* 141.5 (M^{2-}). Anal. Calcd for $C_{24}H_{46}Cu_1Mo_1N_2O_8S_2$: C, 37.66; H, 7.44; N, 7.75; S, 11.83. Found: C, 37.30; H, 7.71; N, 7.80; S, 11.95.

$(Et_4N)_2[O_2MoS_2Cu(SPh)]$ ($(Et_4N)_2$[2]). Method A. An acetonitrile (20 mL) solution of $(Et_4N)_2[Cu(SPh)_3]$ (0.790 g, 1.2 mmol) was added to $(Et_4N)_2[MoO_2S_2]$ (0.434 g, 0.96 mmol) in acetonitrile (20 mL). The solution was stirred at room temperature for 4 h and was then evaporated to dryness. The residue was washed by THF (10 mL, 3 times) and was extracted with acetonitrile (5 mL) at room temperature. The solution was layered with diethyl ether (18 mL) to afford $(Et_4N)_2$[**2**] as yellow-orange plates (0.512 g, 85%). IR (KBr, cm^{-1}): ν(Mo═O) 893, 870, ν(Mo−S−Cu) 455. UV−vis (λ_{max}, nm (ϵ, M^{-1} cm^{-1}), acetonitrile): 232 (sh), 288 (4000), 406 (400). ESI-TOF-MS (acetonitrile): *m*/*z* 182.9 (M^{2-}). ^{1}H NMR (CD_3CN, anion part): δ 7.71 (d, 2H), 6.96 (t, 2H), 6.77 (t, 2H). Anal. Calcd for $C_{24}H_{46}Cu_1Mo_1N_2O_8S_3$: C, 42.26; H, 7.25; N, 4.48; S, 15.38. Found: C, 41.80; H, 6.99; N, 4.67; S, 15.05.

Method B. A mixture of $(Et_4N)_2[O_2MoS_2Cu(CN)]$ (0.648 g, 1.20 mmol) and KSPh (0.196 g, 1.32 mmol) in acetonitrile (20 mL) was stirred for 4 h, giving an orange solution and a white powder. The mixture was centrifuged to remove the white precipitate. The supernatant was diluted with 120 mL of diethyl ether to produce an orange powder $(Et_4N)_2$[**2**] (0.532 g, 71%). Crystalline yellow-orange plates can be obtained from acetonitrile/Et_2O.

$(Et_4N)_2[O_2MoS_2CuS(o\text{-Tol})]$ ($(Et_4N)_2$[3]). This procedure is similar to that for $(Et_4N)_2$[**2**]. Reaction of $(Et_4N)_2[O_2MoS_2Cu(CN)]$ with KS(*o*-Tol) gave the product as a yellow powder. Recrystallization from acetonitrile/^{t}BuOMe afforded $(Et_4N)_2$[**3**] as yellow crystals (56%). IR (KBr, cm^{-1}): ν(Mo═O) 891, 864, ν(Mo−S−Cu) 451. UV−vis (λ_{max}, nm (ϵ, M^{-1} cm^{-1}), acetonitrile): 218 (sh), 278 (11200), 324 (sh), 402 (1700). ^{1}H NMR (CD_3CN, anion): δ 8.05 (d, 1H), 6.96 (d, 1H), 6.84 (t, 1H), 6.71 (t, 1H), 2.41 (s, 3H). Reliable CHNS data could not be obtained because of the highly hygroscopic property of $(Et_4N)_2$[**3**].

$(Et_4N)_2[O_2MoS_2CuS(p\text{-Tol})]$ ($(Et_4N)_2$[4]). To a methanol (10 mL) solution of *p*-TolSH (0.127 g, 1.0 mmol) was added KO^{t}Bu (0.112 g, 1.0 mmol) in methanol (10 mL). The solvent was removed in vacuo, and the residue was dissolved in acetonitrile (20 mL). This solution was added to an acetonitrile (10 mL) solution of $(Et_4N)_2[O_2MoS_2Cu(CN)]$ (0.544 g, 1.0 mmol) at room temperature. The resulting orange slurry was centrifuged to remove KCN. The

(22) Churchill, M. R.; Kalra, K. L. *Inorg. Chem.* **1974**, *13*, 1065.
(23) Comba, P.; Katsichtis, C.; Nuber, B.; Pritzkow, H. *Eur. J. Inorg. Chem.* **1999**, 777.
(24) Jardine, F. H.; Rule, L.; Vohra, G. *J. Chem. Soc., Dalton Trans.* **1970**, 238.

supernatant was diluted with (120 mL) of diethyl ether to produce a yellow powder (0.396 g, 62%), which can be recrystallized from acetonitrile/^{t}BuOMe. IR (KBr, cm^{-1}): ν(Mo═O) 891, 864, ν(Mo−S−Cu) 449. UV−vis (λ_{max}, nm (ϵ, M^{-1} cm^{-1}), acetonitrile): 228 (sh), 288 (14400), 406 (1160). ^{1}H NMR (CD_3CN, anion): δ 7.57 (d, 2H), 6.79 (d, 2H), 2.19 (s, 3H). Reliable CHNS data could not be obtained because of the highly hygroscopic property of $(Et_4N)_2$-[**4**].

$(Et_4N)[O_2MoS_2Cu(PPh_3)]$ ((Et_4N)[5]). To a solution of $(Et_4N)_2$-$[MoO_2S_2]$ (0.889 g, 2.0 mmol) in acetonitrile (40 mL) was added solid $(PPh_3)CuCl$ (0.819 g, 2.3 mmol). As the reaction proceeded, a yellow-orange crystalline powder was formed. The suspension was concentrated in vacuo to ca. 10 mL. The solid material was collected by filtration and was washed with a small amount of acetonitrile and diethyl ether. The product was obtained as a yellow crystalline powder (0.731 g, 58%), which can be recrystallized from acetonitrile at 0 °C. IR (KBr, cm^{-1}): ν(Mo═O) 899, 868, ν(Mo−S−Cu) 455. UV−vis (λ_{max}, nm (ϵ, M^{-1} cm^{-1}), acetonitrile): 272 (13000), 314 (sh), 388 (800). ESI-TOF-MS (acetonitrile): *m*/*z* 518.7 (M$^-$). ^{1}H NMR ($CDCl_3$, anion): δ 7.54−7.51 (m, 6H), 7.38−7.34 (m, 9H). ^{1}H NMR (d_6-DMSO, anion): δ 7.59−7.56 (m, 6H), 7.55−7.50 (m, 9H). ^{31}P{^{1}H} NMR (d_6-DMSO): δ 16.90 (s). Anal. Calcd for $C_{26}H_{35}Cu_1Mo_1N_1O_2P_1S_2$: C, 47.88; H, 5.58; N, 2.25; S, 9.89. Found: C, 48.18; H, 5.44; N, 2.16; S, 9.89.

$(Et_4N)[O_2MoS_2Cu(dppe)]$ ((Et_4N)[6]). This synthetic procedure is analogous to that of (Et_4N)[**5**]. The reaction of $(Et_4N)_2[MoO_2S_2]$ (0.540 g, 1.2 mmol) with $Cu_2I_2(dppe)_3$ (0.944 g, 0.60 mmol) in acetonitrile (30 mL) afforded (Et_4N)[**6**] as a yellow-orange crystalline powder (0.792 g, 85%). Recrystallization from DMF/Et_2O gave (Et_4N)[**6**] as yellow-orange crystals. IR (KBr, cm^{-1}): ν(Mo═O) 887, 864, ν(Mo−S−Cu) 453. UV−vis (λ_{max}, nm (ϵ, M^{-1} cm^{-1}), acetonitrile): 278 (17200), 318 (sh), 440 (800). ESI-TOF-MS (acetonitrile): *m*/*z* 654.7 (M$^-$). ^{1}H NMR (d_6-DMSO, anion): δ 7.62−7.59 (m, 8H), 7.37−7.34 (m, 12H), 2.30 (t, 4H). ^{31}P{^{1}H} NMR (d_6-DMSO): δ −10.7 (s). Anal. Calcd for $C_{34}H_{44}Cu_1$-$Mo_1N_1O_2P_2S_3$: C, 52.07; H, 5.65; N, 1.79; S, 8.18. Found: C, 51.70; H, 5.82; N, 2.01; S, 8.34.

$(Et_4N)[O_2MoS_2Cu(triphos)]$ ((Et_4N)[7]). To a solution of (triphos)CuCl (0.109 g, 0.15 mmol) in CH_2Cl_2 (10 mL) was added $(Et_4N)_2[MoO_2S_2]$ (0.071 g, 0.16 mmol) in MeCN (10 mL) at 0 °C. After the mixture was stirred at 0 °C for 30 min, the solvents were removed in vacuo. The residue was dissolved in MeCN (5 mL) and layered with diethyl ether to form an orange crystal of (Et_4N)-[**7**] (0.072 g, 47%). IR (KBr, cm^{-1}): ν(Mo═O) 887, 870, ν(Mo−S−Cu) 449. UV−vis (λ_{max}, nm (ϵ, M^{-1} cm^{-1}), acetonitrile): 269 (19600), 315 (sh). ESI-TOF-MS (acetonitrile): *m*/*z* 880.3 (M$^-$). ^{1}H NMR (d_6-DMSO, anion): δ 7.77 (br, 12H), 7.30 (br, 18H), 2.78 (br, 6H), 0.59 (br, 3H). ^{31}P{^{1}H} NMR (d_6-DMSO): δ −4.00 (s), −24.49 (s). An analytically pure sample of this compound was not obtained. The orange crystals of (Et_4N)[**7**] are accompanied by a small amount of Et_4NCl; the separation of which was unsuccessful.

$(Et_4N)_2[(1,2\text{-}S_2C_6H_4)Mo(O)S_2Cu(CN)]$ ($(Et_4N)_2$[8]). An acetonitrile (5 mL) solution of benzene-1,2-dithiol (0.0367 g, 0.26 mmol) was added to $(Et_4N)_2[O_2MoS_2Cu(CN)]$ (0.142 g, 0.26 mmol) in acetonitrile (15 mL). The solution immediately turned purple-black. Stirring was continued for 4 h. Solvent was removed under vacuum, and the black-purple residue was washed with a mixture of methanol/Et_2O (1:1) (5 mL, 3 times) to afford a purple powder. Recrystallization from acetonitrile/Et_2O gave $(Et_4N)_2$[**8**] as purple plates (0.114 g, 65%). IR (KBr, cm^{-1}): ν(CN) 2119, ν(Mo═O) 924, ν(Mo−S−Cu) 426. UV−vis (λ_{max}, nm (ϵ, M^{-1} cm^{-1}), acetonitrile): 230 (36000), 254 (38000), 310 (sh), 380 (sh), 530 (1600). ESI-TOF-MS (acetonitrile): *m*/*z* 203.5 (M^{2-}). ^{1}H NMR (CD_3CN, anion): δ 7.31 (dd, 2H), 6.83 (dd, 2H). Anal. Calcd for $C_{24}H_{46}Cu_1Mo_1N_2O_8S_4$: C, 41.46; H, 6.66; N, 6.31; S, 19.25. Found: C, 41.54; H, 6.72; N, 6.24; S, 19.70. Cyclic voltammetry (acetonitrile): $E_{1/2}$ −2.10 (rev), −1.23 (quasi-rev) V.

$(Et_4N)_2[(1,2\text{-}S_2C_6H_4)Mo(O)S_2Cu(SPh)]$ ($(Et_4N)_2$[9]). This procedure is similar to the one used for the synthesis of $(Et_4N)_2$[**8**]. The reaction of $(Et_4N)_2[O_2MoS_2Cu(SPh)]$ (0.188 g, 0.30 mmol) with benzene-1,2-dithiol (0.0447 g, 0.31 mmol) in acetonitrile (15 mL) gave $(Et_4N)_2$[**9**] as a purple solid. Recrystallization from acetonitrile/Et_2O afforded $(Et_4N)_2$[**9**] as purple crystals (0.124 g, 55%). IR (KBr, cm^{-1}): ν(Mo═O) 903, ν(Mo−S−Cu) 422. UV−vis (λ_{max}, nm (ϵ, M^{-1} cm^{-1}), acetonitrile): 230 (38600), 252 (40000), 280 (sh), 320 (sh), 380 (10400), 550 (800). ESI-TOF-MS (acetonitrile): *m*/*z* 245.0 (M^{2-}). ^{1}H NMR (CD_3CN, anion): δ 7.71 (d, 2H), 7.31 (dd, 2H), 7.01 (t, 1H), 6.82 (dd, 3H). Anal. Calcd for $C_{24}H_{46}Cu_1$-$Mo_1N_2O_8S_5$: C, 44.87; H, 6.59; N, 3.74; S, 21.39. Found: C, 44.63; H, 6.73; N, 3.92; S, 21.57. Cyclic voltammetry (acetonitrile): E_{pc} −2.10 (irr), −1.29 (irr) V.

$(Et_4N)_2[(1,2\text{-}S_2C_6H_4)Mo(O)S_2CuS(p\text{-}Tol)]$ ($(Et_4N)_2$[10]). This procedure is similar to that used for the synthesis of $(Et_4N)_2$[**8**]. The reaction of $(Et_4N)_2[O_2MoS_2CuS(p\text{-Tol})]$ (0.646 g, 1.0 mmol) with benzene-1,2-dithiol (0.159 g, 1.2 mmol) in acetonitrile (25 mL) gave a purple solid. Recrystallization from acetonitrile/Et_2O afforded $(Et_4N)_2$[**10**] as purple crystals (0.431 g, 56%). IR (KBr, cm^{-1}): ν(Mo═O) 920, ν(Mo−S−Cu) 418. UV−vis (λ_{max}, nm (ϵ, M^{-1} cm^{-1}), acetonitrile): 230 (8160), 254 (8600), 312 (sh), 384 (sh), 528 (376). ESI-TOF-MS (acetonitrile): *m*/*z* 252.0 (M^{2-}). ^{1}H NMR (CD_3CN, anion): δ 7.57 (m, 2H), 7.31 (m, 2H), 6.84 (m, 4H), 2.22 (s, 3H). Anal. Calcd for $C_{24}H_{46}Cu_1Mo_1N_2O_8S_5$: C, 45.62; H, 6.73; N 3.67; S, 21.00. Found: C, 45.35; H, 6.98; N, 4.14; S, 20.57. Cyclic voltammetry (acetonitrile): E_{pc} −2.13 (irr), −1.32 (irr) V.

$(Et_4N)_2[(1,2\text{-}S_2C_6H_2\text{-}3,6\text{-}Cl_2)Mo(O)S_2Cu(CN)]$ ($(Et_4N)_2$[11]). A solution of 0.110 g (0.20 mmol) of $(Et_4N)_2[O_2MoS_2Cu(CN)]$ in 15 mL of acetonitrile was treated with 0.0441 g (0.21 mmol) of 3,6-dichloro-benzene-1,2-dithiol in 5 mL of THF. The solution turned purple. After the mixture was stirred for 3 h, the solvent was removed in vacuo and the residue was washed with a mixture of methanol/Et_2O (1:1) (5 mL, 3 times). The product was recrystallized from acetonitrile and diethyl ether to afford purple crystals (0.072 g, 48%). IR (KBr, cm^{-1}): ν(CN) 2125, ν(Mo═O) 916, ν(Mo−S−Cu) 430. UV−vis (λ_{max}, nm (ϵ, M^{-1} cm^{-1}): 236 (sh), 262 (19200), 314 (sh), 388 (sh), 532 (660). ESI-TOF-MS (acetonitrile): *m*/*z* 237.5 (M^{2-}). ^{1}H NMR (CD_3CN, anion): δ 6.96 (s, 2H). Anal. Calcd for $C_{24}H_{46}Cu_1Mo_1N_2O_8S_5$: C, 37.57; H, 5.76; N, 5.72; S, 17.44. Found: C, 36.93; H, 5.63; N, 5.55; S, 17.32. Cyclic voltammetry (acetonitrile): $E_{1/2}$ −1.95 (rev), −1.18 (quasi-rev) V.

$(Et_4N)_2[(1,2\text{-}S_2C_6H_2\text{-}3,6\text{-}Cl_2)Mo(O)S_2Cu(SPh)]$ ($(Et_4N)_2$[12]). This procedure is similar to the one used for the synthesis of $(Et_4N)_2$-[**11**]. The reaction of $(Et_4N)_2[O_2MoS_2Cu(SPh)]$ (0.129 g, 0.21 mmol) with 3,6-dichloro-benzene-1,2-dithiol (0.0439 g, 0.21 mmol) in acetonitrile (20 mL) and THF (10 mL) gave a purple solid. Recrystallization from acetonitrile/Et_2O afforded $(Et_4N)_2$[**12**] as purple crystals (0.064 g, 37%). IR (KBr, cm^{-1}): ν(Mo═O) 912, ν(Mo−S−Cu) 426. UV−vis (λ_{max}, nm (ϵ, M^{-1} cm^{-1}), acetonitrile): 238 (sh), 260 (31800), 324 (sh), 368 (9800), 562 (800). ESI-TOF-MS (acetonitrile): *m*/*z* 278.7 (M^{2-}). ^{1}H NMR (CD_3CN, anion): δ 7.69 (d, 2H), 7.01 (t, 2H), 6.96 (s, 2H), 6.84 (t, 1H). Anal. Calcd for $C_{28}H_{47}Cu_1Mo_1N_2O_8S_5$: C, 41.09; H, 5.79; N, 3.42; S, 19.59. Found: C, 40.72; H, 5.68; N, 3.85; S, 19.65.

Table 5. Crystal Data for $(Et_4N)_2$[**2**−**4**, **8**−**10**, **12**, and **13**] and (Et_4N)[**5**−**7**]

	$(Et_4N)_2$[**2**]	$(Et_4N)_2$[**3**]	$(Et_4N)_2$[**4**]	(Et_4N)[**5**]	(Et_4N)[**6**]	(Et_4N)[**7**]
formula	$C_{22}H_{45}Cu_1Mo_1N_2O_2S_3$	$C_{23}H_{47}Cu_1Mo_1N_2O_2S_3$	$C_{23}H_{47}Cu_1Mo_1N_2O_2S_3$	$C_{26}H_{35}Cu_1Mo_1N_1O_2P_1S_2$	$C_{34}H_{44}Cu_1Mo_1N_1O_2P_2S_2$	$C_{49}H_{59}Cu_1Mo_1N_1O_2P_3S_2$
mol wt (g mol^{-1})	625.30	639.32	639.32	648.16	784.29	1010.55
cryst syst	monoclinic	monoclinic	monoclinic	orthorhombic	monoclinic	triclinic
space group	*C*2 (No. 5)	*C*2 (No. 5)	*C*2 (No. 5)	*Pca*2$_1$ (No. 29)	*P*2$_1$/*c* (No. 14)	*P*-1 (No. 2)
cryst color	yellow	yellow	yellow	yellow	orange	orange
a (Å)	15.928(8)	16.015(6)	16.144(4)	18.646(8)	11.458(1)	10.420(4)
b (Å)	8.755(4)	8.791(3)	8.609(2)	13.908(6)	16.502(2)	10.716(4)
c (Å)	20.77(1)	23.928(9)	21.838(6)	10.826(5)	18.804(2)	23.310(8)
α (deg)						93.974(9)
β (deg)	96.055(6)	104.712(4)	96.127(5)		95.055(2)	90.616(8)
γ (deg)						92.860(8)
V (Å^3)	2880(2)	3258(1)	3017.6(1)	2807(4)	3541(6)	2593.0(1)
Z	4	4	4	4	4	2
ρ_{calcd} (g cm^{-3})	1.442	1.303	1.407	1.477	1.471	1.294
$2\theta_{max}$ (deg)	55	55	55	55	55	55
no. of unique rflns	4362	3928	3677	3383	8041	11407
no. of obsd rflns[a]	6001	3921	3662	3371	8004	6061
no. of parameters	279	289	289	307	388	532
R[b]	0.055	0.067	0.050	0.023	0.029	0.061
Rw[c]	0.069	0.089	0.057	0.024	0.035	0.087
GOF[d]	1.38	2.40	0.82	0.90	1.29	1.42

	$(Et_4N)_2$[**8**]	$(Et_4N)_2$[**9**]	$(Et_4N)_2$[**10**]	$(Et_4N)_2$[**12**]	$(Et_4N)_2$[**13**]
formula	$C_{23}H_{44}Cu_1Mo_1N_3OS_4$	$C_{28}H_{49}Cu_1Mo_1N_2OS_5$	$C_{29}H_{51}Cu_1Mo_1N_2OS_5$	$C_{28}H_{47}Cu_1Mo_1N_2O_1S_5Cl_2$	$C_{24}H_{49}Cu_1Mo_1N_2O_1S_5$
mol wt (g mol^{-1})	666.35	749.526	763.52	818.38	701.45
cryst system	orthorhombic	monoclinic	monoclinic	monoclinic	orthorhombic
space group	*Pbca* (No. 61)	*P*2$_1$/n (No. 14)	*P*2$_1$/c (No. 14)	*C*2 (No. 5)	*Pbca* (No. 61)
cryst color	purple	purple	purple	dark-purple	dark-purple
a (Å)	14.843(3)	9.286(3)	17.831(9)	15.678(7)	15.047(3)
b (Å)	13.790(3)	29.31(1)	12.226(6)	10.890(4)	14.072(2)
c (Å)	29.128(7)	12.483(4)	17.806(9)	21.376(9)	30.353(5)
α (deg)					
β (deg)		95.644(4)	117.036(5)	95.278(5)	
γ (deg)					
V (Å^3)	5962(2)	3380(2)	3457(2)	3634(2)	6427(3)
Z	8	4	4	4	8
ρ_{calcd} (g cm^{-3})	1.485	1.535	1.467	1.496	1.450
$2\theta_{max}$ (deg)	55	55	55	55	55
no. of unique rflns	5924	7582	5046	5303	3105
no. of obsd rflns[a]	6791	4710	6678	5303	3105
no. of parameters	334	343	352	361	307
R[b]	0.087	0.056	0.080	0.039	0.081
Rw[c]	0.093	0.066	0.082	0.040	0.089
GOF[d]	1.84	1.04	1.03	1.00	1.73

[a] Observation criterion $I > 3\sigma(I)$. [b] $R = \sum||F_o| - |F_c||/\sum|F_o|$. [c] $Rw = [\{\sum w(|F_o| - |F_c|)^2\}/\sum wF_o^2]^{1/2}$. [d] $GOF = [\{\sum w(|F_o| - |F_c|)^2\}/(N_o - N_p)]^{1/2}$, where N_o and N_p denote the number of data and parameters.

$(Et_4N)_2$[(1,2-$S_2C_2H_4$)Mo(O)S_2Cu(SPh)] ($(Et_4N)_2$[13]). A solution of 0.230 g (0.37 mmol) of $(Et_4N)_2[O_2MoS_2Cu(SPh)]$ in 20 mL of acetonitrile was treated with 0.035 mL (0.42 mmol) of 1,2-ethanedithiol in 10 mL of acetonitrile. The solution turned purple. After the mixture was stirred for 4 h, the solvent was removed in vacuo and the residue was washed with a mixture of methanol/Et_2O (1:1) (5 mL, 3 times). The product was recrystallized from acetonitrile and diethyl ether to give purple crystals 0.086 g (33%). IR (KBr, cm^{-1}): ν(Mo═O) 916, ν(Mo−S−Cu) 422. UV−vis (λ_{max}, nm (ϵ, M^{-1} cm^{-1}), acetonitrile): 284 (13940), 364 (8800), 574 (880). ESI-TOF-MS (acetonitrile): *m*/*z* 220.9 (M^{2-}). ^{1}H NMR (CD_3CN, anion): δ 7.70 (d, 2H), 6.99 (t, 2H), 6.81 (t, 1H), 3.06 (bs, 4H). Anal. Calcd for $C_{24}H_{49}Cu_1Mo_1N_2O_8S_5$: C, 41.09; H, 7.04; N, 3.99; S, 22.86. Found: C, 40.64; H, 7.27; N, 4.18; S, 23.30. Cyclic voltammetry (acetonitrile): E_{pc} −2.33 (irr) V.

X-ray Crystal Structure Determination. Crystal data and refinement parameters for the structurally characterized complexes are summarized in Table 5. Single crystals were coated with oil (Immersion Oil, type B, code 1248, Cargille Laboratories, Inc.) and mounted on loops. Diffraction data were collected at −100 °C under a cold nitrogen stream on a Rigaku AFC7 equipped with a Mercury CCD area detector (for **2**, **3**, **5**, **6**, **9**, **10**, and **11**), on a Rigaku AFC8 equipped with a Saturn 70 CCD area detector (for **7**, **8**, **12**, and **13**), or a Rigaku RA-Micro7 with a Saturn 70 with MicroMax-007 CCD area detector (for **4**) using graphite-monochromated Mo Kα radiation (λ = 0.710690 Å). Four preliminary data frames were measured at 0.5° increments of ω, to assess the crystal quality and preliminary unit cell parameters. The intensity images were also measured at 0.5° intervals of ω. The frame data were integrated using the CrystalClear program package, and the data sets were corrected for absorption using a REQAB program. The calculations were performed with the TEXSAN program package. All of the structures were solved by a direct method and refined by full-matrix least squares. Anisotropic refinement was

applied to all of the non-hydrogen atoms, and all of the hydrogen atoms were put at the calculated positions.

Acknowledgment. This research was financially supported by Grants-in-Aids for Scientific Research (No. 14078211 and 15750047) from the Ministry of Education, Culture, Sports, Science and Technology, Japan and by the 21st COE program (Establishment of COE on Materials Science: Elucidation and Creation of Molecular functions). The authors thank Prof. Josef Takats at University of Alberta for his comments.

Supporting Information Available: Crystallographic data for **2** and **7**−**9** (CIF) or **3**−**6**, **10**, **12**, and **13** (CIF and PDF), and cyclic voltammogram of **8**−**11**. This material is available free of charge via the Internet at http://pubs.acs.org.

IC050294V